

Article

Molecular and Segmental Orientational Order in a Smectic Mesophase of a Thermotropic Ionic Liquid Crystal

Jing Dai ¹, Boris B. Kharkov ² and Sergey V. Dvinskikh ^{1,2,*} ¹ Department of Chemistry, KTH Royal Institute of Technology, SE-10044 Stockholm, Sweden; jdai@kth.se² Laboratory of Biomolecular NMR, Saint Petersburg State University, Saint Petersburg 199034, Russia; st036820@student.spbu.ru

* Correspondence: sergeid@kth.se; Tel.: +46-8-790-82-24

Received: 30 November 2018; Accepted: 24 December 2018; Published: 28 December 2018



Abstract: We investigate conformational dynamics in the smectic A phase formed by the mesogenic ionic liquid 1-tetradecyl-3-methylimidazolium nitrate. Solid-state high-resolution ¹³C nuclear magnetic resonance (NMR) spectra are recorded in the sample with the mesophase director aligned in the magnetic field of the NMR spectrometer. The applied NMR method, proton encoded local field spectroscopy, delivers heteronuclear dipolar couplings of each ¹³C spin to its ¹H neighbours. From the analysis of the dipolar couplings, orientational order parameters of the C–H bonds along the hydrocarbon chain were determined. The estimated value of the molecular order parameter *S* is significantly lower compared to that in smectic phases of conventional non-ionic liquid crystals.

Keywords: ionic liquids; liquid crystals; ionic liquid crystals; molecular orientational order; nuclear magnetic resonance

1. Introduction

Ionic liquids that form ordered mesophases in temperature ranges between solid and isotropic liquid phases belong to a class of ionic liquid crystal (ILC) materials [1]. Molecules and ions in liquid crystals (LC) exhibit a high molecular translational and rotational mobility combined with orientational and positional order. The unique synergy of ionic conductivity and anisotropic nanoscale structure makes ILC materials in high demand in the development of low-dimensional charge transport technology and other applications [2].

Nuclear magnetic resonance (NMR) spectroscopy is widely used to study molecular conformational and rotational dynamics and orientational order in LC [3,4]. Site-specific information at the atomic level can be obtained by high resolution ¹³C NMR combined with selective suppression of spin interactions. Structural and order parameters are obtained through the measurements of orientation- and distance-dependent dipole couplings. Due to the orientational ordering, the dipolar coupling in mesophase is not averaged to zero, in contrast to isotropic phase. ¹³C–¹H heteronuclear dipolar couplings in LC are measured by two-dimensional (2D) separated local field spectroscopy technique [5].

The local bond order parameter *S*_{CH} characterizes the average orientation of the C–H bond to the LC director. The ratio of the residual dipolar coupling averaged by the anisotropic motion, to its unaveraged value provides the *S*_{CH}. For molecules with long hydrocarbon chains one can study a C–H bond order parameter profile, a variation of *S*_{CH} along the chain, which characterizes the average molecular structure in the mesophase [6–8].

Here we investigate conformation and molecular order of organic cations in the smectic A phase of the mesogenic ionic liquid 1-tetradecyl-3-methylimidazolium nitrate (C₁₄mimNO₃) [9].

The sample forms interdigitated bilayer structures where the molecules, consisting of non-ionic and ionic non-miscible parts, phase-separate at the nanoscale. Relatively low transition temperatures between meso- and isotropic phases and a wide temperature range of the mesophase existence make this sample particularly suitable for preparing it both in un-aligned state and with director aligned with respect to external magnetic field. In the latter case, the sample is suitable for studies by high-resolution solid-state NMR at stationary condition (without sample spinning). We apply 2D ^{13}C - ^1H dipolar NMR spectroscopy to the Smectic A phase of the $\text{C}_{14}\text{mimNO}_3$ to quantitatively characterize the molecular dynamics. Based on the profiles of the order parameters obtained, we put forward a model for the motion of the organic cations in the bilayer of the smectic A phase.

2. Materials and Methods

The sample of $\text{C}_{14}\text{mimNO}_3$ (1-tetradecyl-3-methylimidazolium nitrate, CAS 799246-94-9) was obtained from Angene International and used as received. Water content in the sample was estimated to ≈ 1.0 wt.% from ^1H NMR spectrum recorded in the isotropic phase. No other significant impurity signals were observed. The sample exhibited the following phase transition temperatures: Isotropic $\xrightarrow{+129\text{ }^\circ\text{C}}$ Smectic A $\xrightarrow{+43\text{ }^\circ\text{C}}$ Crystal, as observed by recording proton NMR spectra. Transition temperature to the smectic phase is in agreement with reported phase diagram [9]. Slightly higher crystallization temperature compared to that determined by differential scanning calorimetry in [9] is presumably due to much slower cooling rate applied in our NMR experiments. Upon slow cooling from the isotropic phase in the presence of the strong external magnetic field, director of the smectic phase is aligned perpendicular to the magnetic field vector. Most of our experiments were performed in such an oriented sample. To produce random director orientation in the smectic phase, the sample was cooled from the isotropic phase while out of the magnet. Due to the high viscosity of the smectic phase, the domains of different orientations do not reorient when the sample in the smectic phase is placed in magnetic field.

Experiments were performed using Bruker 500 Avance III spectrometer at Larmor frequencies of 500.1 and 125.7 for ^1H and ^{13}C , respectively. About 0.5 g of the sample was loaded in a standard 5 mm NMR tube. NMR spectra were recorded using solution state multinuclear 5 mm probe-head. The ^1H and ^{13}C 90° -pulse lengths were 8 and 13 μs , respectively. For heteronuclear proton decoupling in the mesophase, Spinal64 sequence [10] with the ^1H nutation frequency of 23 kHz was used during acquisition time of 120 ms. To enhance the intensity of the ^{13}C signal, proton-to-carbon cross polarization (CP) with adiabatic demagnetization in the rotating frame (ADRF) [11] was applied with nutation frequencies up to 16 kHz and contact time in the range 10–20 ms.

Dipolar ^1H - ^{13}C spectra were recorded using proton detected/encoded local field (PDLF) NMR spectroscopy [12]. The PDLF spectrum is governed by a two-spin interaction and thus cross sections in the indirect dimension present superposition of dipolar doublets. The actual PDLF pulse sequence is shown in the Supplementary Materials, Figure S2. The evolution time in indirect time domain was incremented with 384 μs in 256 steps, at each with four collected transients. Proton homonuclear decoupling during the evolution time was achieved by the BLEW-48 multiple-pulse sequence [13] with a nutation frequency of 31.2 kHz.

The temperature was regulated with an accuracy of 0.1 $^\circ\text{C}$. The temperature shift and temperature gradient within the sample, caused by the decoupling irradiation, were calibrated by observing the change in the ^{13}C spectral line widths and positions. Decoupling power, irradiation time, and repetition delay were adjusted to limit heating effects to <0.5 $^\circ\text{C}$.

3. Results and Discussion

3.1. Carbon-13 Nuclear Magnetic Resonance (NMR) Spectra

Representative ^{13}C NMR spectra of the C_{14}mim ions in different phases are displayed in Figure 1. All carbons, except carbons 5 and 6 with overlapped signals, were resolved. The assignment of the carbon signals in the isotropic and mesophase was verified, respectively, by the INADEQUATE (incredible natural-abundance double-quantum transfer) experiment [14] and by dipolar INADEQUATE experiment as described in Supplementary Materials. The chemical shifts of the corresponding signals in the spectra in Figure 1a,b reflect different parts of residual chemical shift anisotropy (CSA) tensor. The signal positions in the isotropic phase are given by the isotropic averages δ_i of the respective CSA tensors. In the spectrum in the aligned mesophase, (Figure 1b), the chemical shift corresponds to one of the principal values $\delta_{\alpha\alpha}$ ($\alpha = x, y, z$) of the residual CSA tensor.

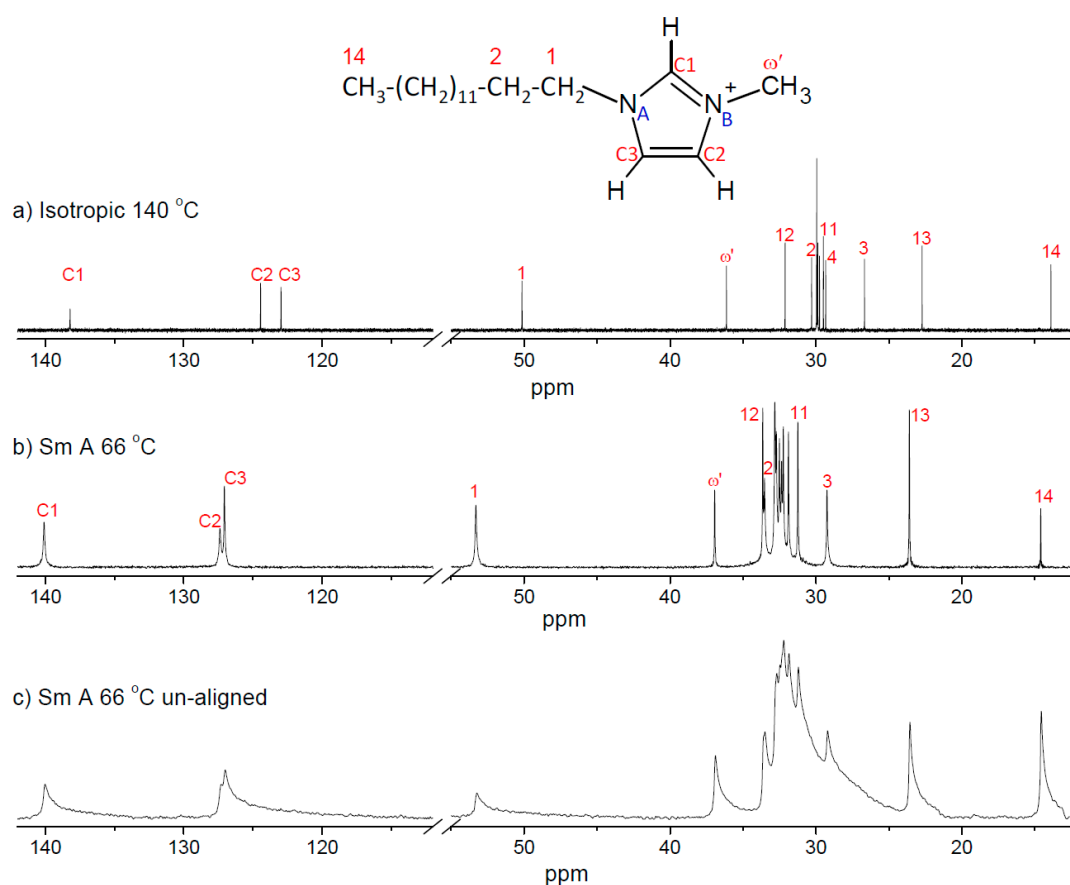


Figure 1. ^{13}C nuclear magnetic resonance (NMR) spectra of $\text{C}_{14}\text{mimNO}_3$ in the isotropic (a) and smectic A phase (b,c) at indicated temperatures. The spectrum (c) was recorded in the un-aligned smectic A phase.

In uniaxial liquid crystals, the chemical shift tensor is described by the components along and orthogonal to the phase director, δ_{\parallel}^{LC} and δ_{\perp}^{LC} , respectively. In our sample, which exhibits a negative anisotropy of the diamagnetic susceptibility, the director aligns in the plane perpendicular to the magnetic field of the spectrometer. Hence, the observed chemical shifts are determined by the δ_{\perp}^{LC} values. This is verified comparing the spectrum of the aligned sample in Figure 1b to the spectrum of the sample prepared with random director distribution, Figure 1c. The random director alignment was achieved by cooling the sample from the isotropic phase outside the NMR magnet. The chemical shifts corresponding to the edges of the axially symmetric CSA patterns observed in un-aligned sample, match those of the respective lines in the aligned mesophase.

3.2. ^1H - ^{13}C Dipolar Spectra

The 2D PDLF spectrum at 66 °C is shown in Figure 2a. The cross sections in the dipolar direction for different carbons are shown in Figure 2b. The dipolar splittings between directly bound ^{13}C and ^1H spins are well resolved and can be directly measured in the spectrum for each carbon in the molecule. Additional low intensity doublets observed for some of the dipolar cross-sections, e.g., in the spectrum of the chain carbon 2, are due to partial overlap with nearby signals in the 2D spectrum. The inner multiplets with small splittings resolved for some carbon sites arise from couplings to remote protons in neighbouring groups.

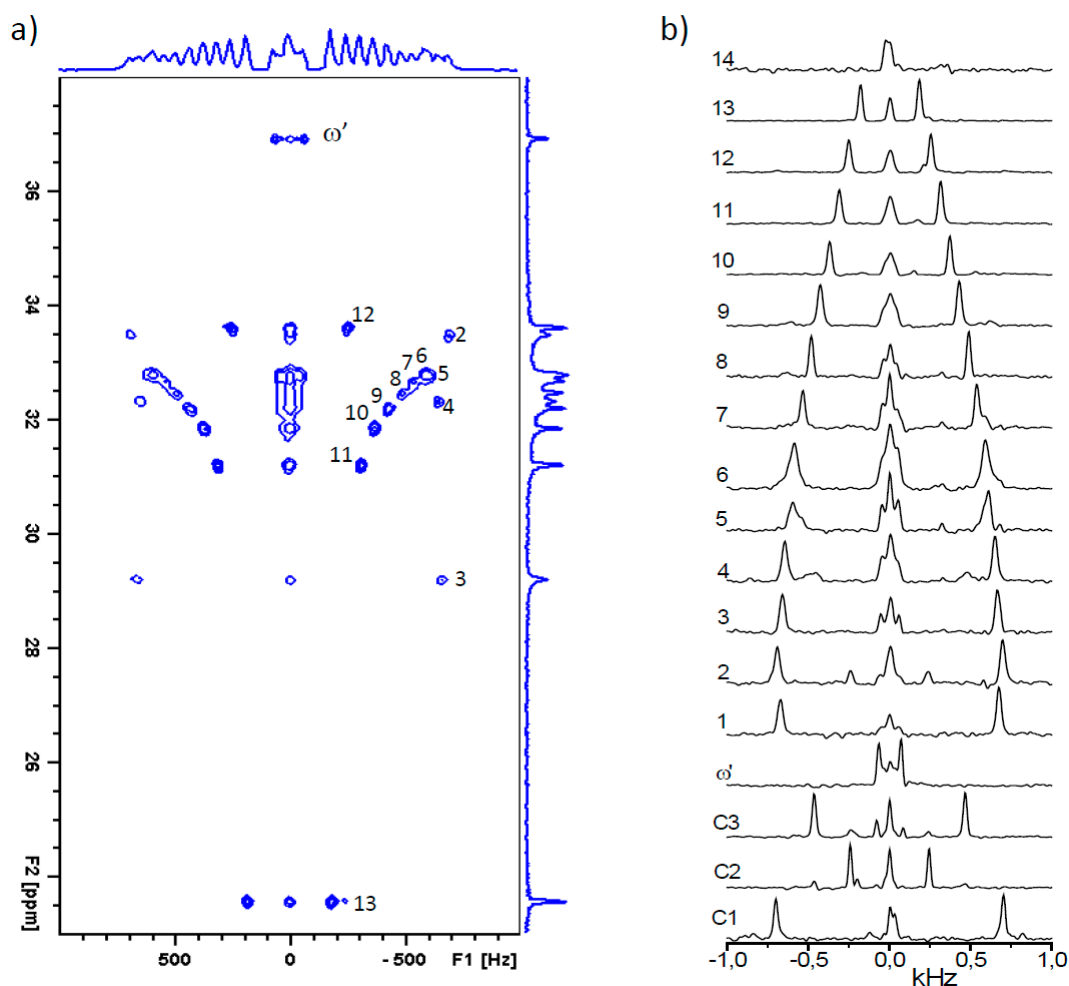


Figure 2. (a) Part of 2D proton detected/encoded local field (PDLF) spectrum in $\text{C}_{14}\text{mimNO}_3$ smectic A phase at 66 °C. (b) Cross-sections along dipolar dimension are shown for all carbons. For spectral assignment, see molecular structure in Figure 1.

The dipole–dipole spin couplings are orientation- and interatomic distances dependent. Anisotropic molecular motion results in partial averaging of the intramolecular dipolar interactions over the conformational dynamics, molecular reorientations, and the molecular axis fluctuations about the mesophase director. Intermolecular spin couplings are averaged to zero by translational dynamics [15]. Different motional modes can often be considered uncorrelated and their effects on spin interactions can be separated. A simplified description of orientational ordering can be applied considering an approximately cylindrical symmetry due to fast uniaxial rotations of elongated

mesogenic molecules [16]. For a ^1H – ^{13}C spin pair in a molecule in an anisotropic phase the dipolar coupling is:

$$d_{CH} = b_{CH} \langle P_2(\cos \theta_{PL}) \rangle \quad (1)$$

with $P_2(\cos \theta_{PL}) = (3 \cos^2 \theta_{PL} - 1)/2$, where θ_{PL} is the angle between the C–H vector, which defines a principal frame axis P of the dipolar interaction, and the magnetic field \mathbf{B}_0 (defines the laboratory frame axis L). The dipolar coupling constant in the principal frame $b_{CH} = -(\mu_0/8\pi^2)(\gamma_H\gamma_C\hbar/r_{CH}^3)$ can be estimated from the atomic distances r_{CH} and the gyromagnetic ratios γ_H, γ_C . For a single C–H bond with account for vibration effects we accept b_{CH} values of -21.5 kHz and -22 kHz for aliphatic and aromatic sites, respectively [17,18].

Anisotropic molecular mobility leads to a partial averaging of the angular term $\langle P_2(\cos \theta_{PL}) \rangle$. Dynamic molecular disorder in LC is measured by the molecular orientational order parameter $S = \langle P_2(\cos \theta_{MN}) \rangle$, where θ_{MN} is the instantaneous angle between the long molecular axis M and the director N . Similarly, the orientational averaging of the local C–H bond direction with the respect to director is described by the bond order parameter $S_{CH} = \langle P_2(\cos \theta_{PN}) \rangle$, where θ_{PN} is the angle between the inter-nuclear vector P and the director N . Thus,

$$d_{CH} = b_{CH} S_{CH} P_2(\cos \theta_{NL}) \quad (2)$$

where θ_{NL} is the angle between director and magnetic field vector. Hence, local bond order parameters S_{CH} can be estimated directly from the NMR dipolar spectra. Assuming statistical independence and large time-scale separation of molecular reorientation and conformational dynamics, the bond order parameters S_{CH} can be related to the molecular order parameter S by the expression:

$$S_{CH} = \langle P_2(\cos \theta_{PM}) \rangle S \quad (3)$$

where θ_{PM} defines the angle between the bond vector and molecular axis. Thus, Equation (2) can be expanded:

$$d_{CH} = b_{CH} \langle P_2(\cos \theta_{PM}) \rangle S P_2(\cos \theta_{NL}) \quad (4)$$

For non-rigid molecules, the separation of the terms $\langle P_2(\cos \theta_{PM}) \rangle$ and S requires some model assumptions of molecular conformational dynamics.

The splitting $\Delta\nu$ observed in the PDLF experiment is contributed by residual dipolar coupling d_{CH} and isotropic indirect spin coupling J_{CH} :

$$\Delta\nu = k(2d_{CH} + J_{CH}) \quad (5)$$

(anisotropic part of indirect coupling ΔJ_{CH} is neglected compared with dipolar coupling [16]). Upon application of homonuclear decoupling both these interactions are scaled down. For the pulse sequence BLEW48 [13], the scaling factor was experimentally calibrated to $k = 0.418 \pm 0.02$.

The magnitudes of the isotropic coupling J_{CH} were measured in the isotropic phase by recording ^{13}C NMR spectrum without proton decoupling. The sign of J_{CH} is known to be positive. Note that the sign of the splitting $\Delta\nu$ is not obtained in the PDLF experiment. However, the sign of the dipolar coupling d_{CH} can be determined from Equation (4) considering average orientation of molecular axis in the magnetic field and C–H bond angles with respect to molecular axis. The dipolar coupling constant in the principal frame b_{CH} is negative for a proton-carbon pair. The molecular order parameter S is positive. The term $P_2(\cos \theta_{NL}) = -0.5$ for the director aligned perpendicular to the magnetic field. The sign of the angular term $P_2(\cos \theta_{PM})$ can be deduced by considering molecular geometry as discussed below.

3.3. Order Parameters

With dipolar couplings d_{CH} obtained from Equation (5), local bond order parameters S_{CH} are directly calculated using Equation (2). With some assumptions about the direction of the molecular axis, as discussed below, molecular order parameter S can as well be estimated from Equation (3). Thus, the analysis on the PDLF spectra provides quantitative information on the local and molecular order parameters, S_{CH} and S .

The variations of S_{CH} along the alkyl chain, or order parameter profiles, are plotted in Figure 3 for selected temperatures in the smectic A phase. The S_{CH} values are negative assuming the average orientation of the C–H bond perpendicular to the direction of long molecular axis. As expected, the methylene groups close to the imidazolium core are less disordered and segmental mobility increases gradually towards the chain terminal methyl. While this average character of the chain dynamics persists in the whole temperature range of the smectic phase, the alkyl chains become more ordered at lower temperatures.

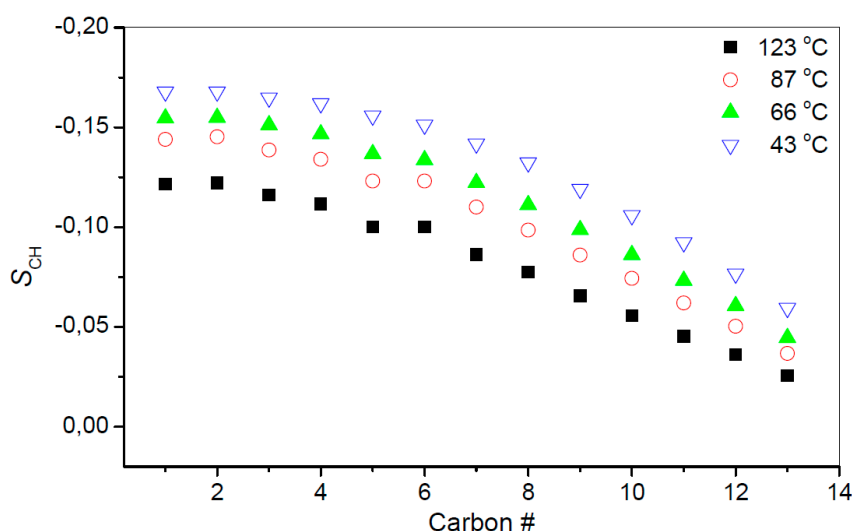


Figure 3. C–H bond order parameter S_{CH} profiles for the alkyl chain of the cation in the smectic A phase of $C_{14}mimNO_3$.

The S_{CH} magnitudes are small and similar to those typically found in lyotropic lamellar phases [8]. It is interesting that S_{CH} values obtained by MD simulation for $C_{16}mimNO_3$ homologue were also found to be similarly small [19]. The low values of S_{CH} , on one hand, may indicate a significant conformational dynamics by trans-gauche isomerisation. The fast decrease of S_{CH} towards chain terminal suggests a gradual intensification of the conformational mobility with increasingly significant population of gauche conformers. On the other hand, limited variation of the order parameters for the first few methylene groups close to the imidazolium core suggests a restricted conformational dynamics for this part of the chain with predominant trans conformation. In this case, relatively small observed values of S_{CH} parameters for the carbons in vicinity of the head group can be due to either a low value of the molecular order parameter S (cf. Equation (3)) or a significant tilt angle of this part of the chain with respect to main molecular axis oriented along the director. Based on this observation, we consider the following model of average molecular conformation in the further analysis: the part of the chain in vicinity of the head group is predominantly in the trans conformation and the symmetry axis of this chain fragment does not significantly deviate from the long molecular axis. The latter assumption is, in fact, supported by the values of S_{CC} order parameters, estimated from the $^{13}C_n-^{13}C_{n+2}$ dipolar couplings for the chain carbons separated by two bonds. The coupling constants were obtained from the dipolar INADEQUATE experiment described in the Supplementary Materials. The estimated magnitude of the order parameters $S_{CC} \approx 0.31$ at 66 °C (averaged value

over methylene segments 1 to 5) is a factor of two larger than the corresponding value $S_{CH} \approx -0.16$. The ratio $S_{CC}/S_{CH} \approx -2$ is indeed expected for C_n-C_{n+2} and C–H vectors, respectively, along and perpendicular to the molecular axis, and thus the model assumption is corroborated.

Within this approach, for the methylenes close to the head group the angular term is $P_2(\cos \theta_{PM}) \approx -0.5$. The molecular order parameter S is, thus, estimated using Equation (4). Temperature dependence $S(T)$ is displayed in Figure 4b, while temperature dependencies of the local bond order parameters for the imidazolium core and for the selected carbons in the chain are shown in Figure 4a. We conclude that the ionic smectic A phase is formed (counter-intuitively) with significantly lower value of the molecular order parameter S when comparing to non-ionic smectic mesogens [20–22]. Theoretical and computational studies suggest that, in contrast to neutral mesogens, the orientational ordering is less important for the stabilization of the smectic layers in ILC where dominant stabilizing effect is due to a "charge-ordered" nanoscale segregation induced by ionic interactions [1,19,23,24].

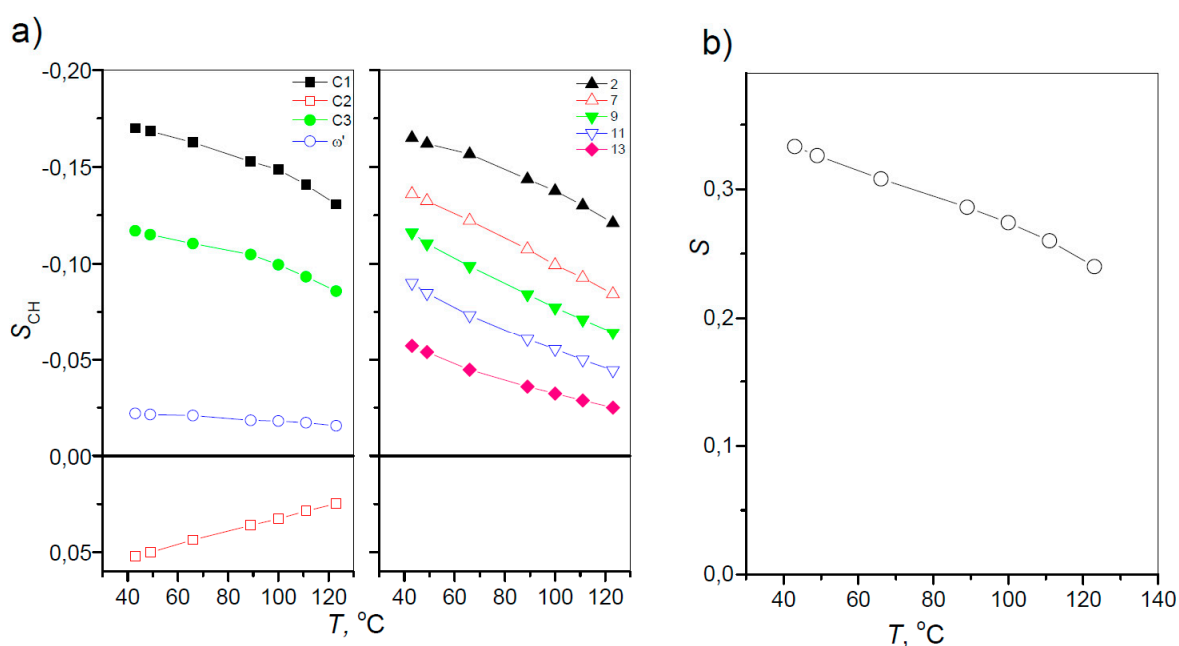


Figure 4. (a) Temperature dependencies of the local bond order parameters S_{CH} for the imidazolium core and selected carbons in the chain in the smectic A phase of $C_{14}mimNO_3$. (b) Temperature dependence of the molecular order parameter S .

In order to analyse the dipolar couplings and local bond order parameters in the imidazolium core (Figure 4a), the molecular axis alignment to imidazolium ring plane has to be correctly accounted for. The planar molecular structure as displayed in Figure 1 is not consistent with the observed couplings in the imidazolium core. In fact, it has been shown by density functional theory (DFT) analysis of similar compounds that in the energy optimized equilibrium structure of C_nmim cations there is a significant angle between the core plane and the symmetry axis of the all-trans aliphatic chain [25]. Non-planar molecular structure is also consistent with recent molecular dynamics (MD) simulation data [19]. A rotation/flip of the imidazolium core around N–C bond can also be accompanied by the chain re-alignment. The correlation of motion by ion-pairing, as has been observed in isotropic phase of ionic liquids, may impose additional restriction on the core dynamics [26–29]. On the other hand, diffusion and conductivity studies have indicated (partial) dissociation of cations and anions in mesophases [28–30]. With reservations for the complexity of the processes controlling the core alignment and dynamics, it is still possible to make rough estimates of the order parameters using DFT structure analysis as presented in [19]. Application of Equation (3) using the direction angles given

in [19] results in S_{CH} estimates of -0.14 , $+0.04$, and -0.07 for the carbons C1, C2, and C3, respectively, (at $66\text{ }^{\circ}\text{C}$) in rough agreement with our experimental results (Figure 4a).

4. Conclusions

In the presented work, the molecular and conformational dynamics of flexible organic cations in the smectic A phase of the ionic liquid $\text{C}_{14}\text{mimNO}_3$ was studied by means of ^1H - ^{13}C dipolar NMR. We demonstrated that the solid-state dipolar NMR spectroscopy in ILC samples is a powerful tool sensitive to details of the molecular conformation and dynamics in the organic smectic layer. The approach does not require isotope labelling; the measurements are performed in samples with natural isotopic abundance. With the sample director aligned in the magnetic field of the spectrometer, the solid-state high-resolution NMR spectra can be obtained in a stationary sample without the necessity of using a magic angle spinning technique.

The obtained experimental data are consistent with the model of the chains preferentially aligned with the layer normal and characterized by relatively low values of the orientational order parameters. Within the temperature interval of the smectic phase, the molecular order parameter S is in the range of 0.25 – 0.35 , which is in approximate agreement with the results of MD analysis of the C16-homologue sample [19,31]. The high rotational/conformational mobility of the organic component in the smectic phase is also accompanied by fast translational displacement as has been shown in experimental and computational diffusion studies of structurally similar ILC [30,32]. Thus, this and previous studies prove highly dynamic behaviour of organic cations in smectic bilayers in ILC.

Supplementary Materials: The following are available online at <http://www.mdpi.com/2073-4352/9/1/18/s1>, Figure S1: Temperature dependent ^{13}C NMR spectra of $\text{C}_{14}\text{mimNO}_3$ in isotropic and smectic A phase. Figure S2: PDLF pulse sequence to record dipolar ^{13}C - ^1H spectra. Figure S3: Dipolar INADEQUATE spectrum in smectic A phase of $\text{C}_{14}\text{mimNO}_3$. Table S1: ^{13}C - ^{13}C dipolar splittings and dipolar couplings for alkyl chain carbons separated by two bonds.

Author Contributions: S.V.D. designed and proposed the methods. J.D. and S.V.D. performed the NMR measurements. B.B.K. performed the numerical analysis. All authors contributed to the preparation of the manuscript.

Funding: This work was supported by the Swedish Research Council VR and by the Russian Foundation for Basic Research (project no. 17-03-00057).

Conflicts of Interest: The authors declare no conflict of interest.

References

1. Goossens, K.; Lava, K.; Bielawski, C.W.; Binnemans, K. Ionic liquid crystals: Versatile materials. *Chem. Rev.* **2016**, *116*, 4643–4807. [[CrossRef](#)] [[PubMed](#)]
2. Kato, T.; Yoshio, M.; Ichikawa, T.; Soberats, B.; Ohno, H.; Funahashi, M. Transport of ions and electrons in nanostructured liquid crystals. *Nat. Rev. Mater.* **2017**, *2*, 17001. [[CrossRef](#)]
3. Dong, R.Y. *Nuclear Magnetic Resonance Spectroscopy of Liquid Crystals*; World Scientific: London, UK, 2010.
4. Dvinskikh, S.V.; Sandström, D.; Zimmermann, H.; Maliniak, A. Carbon-13 NMR Spectroscopy applied to columnar liquid crystals. *Progr. Nucl. Magn. Reson. Spectrosc.* **2006**, *48*, 85–107. [[CrossRef](#)]
5. Dvinskikh, S.V. Characterization of Liquid-Crystalline Materials by Separated Local Field Methods. In *Modern Methods in Solid-State NMR: A practitioners' Guide*; Hodgkinson, P., Ed.; Royal Society of Chemistry: Abingdon, UK, 2018.
6. Boden, N.; Clark, L.D.; Bushby, R.J.; Emsley, J.W.; Luckhurst, G.R.; Stockley, C.P. A deuterium N.M.R. study of chain ordering in the liquid crystals 4,4'-di-n-heptyloxyazoxybenzene and 4-n-octyl-4'-cyanobiphenyl. *Mol. Phys.* **1981**, *42*, 565–594. [[CrossRef](#)]
7. Dvinskikh, S.V.; Castro, V.; Sandström, D. Probing segmental order in lipid bilayers at variable hydration levels by amplitude- and phase-modulated cross-polarization NMR. *Phys. Chem. Chem. Phys.* **2005**, *7*, 3255–3257. [[CrossRef](#)] [[PubMed](#)]
8. Kharkov, B.B.; Chizhik, V.I.; Dvinskikh, S.V. Low RF power high resolution ^1H - ^{13}C - ^{14}N Separated local field spectroscopy in lyotropic mesophases. *J. Magn. Reson.* **2012**, *223*, 73–79. [[CrossRef](#)] [[PubMed](#)]

9. Guillet, E.; Imbert, D.; Scopelliti, R.; Bunzli, J.C.G. Tuning the emission color of europium-containing ionic liquid-crystalline phases. *Chem. Mater.* **2004**, *16*, 4063–4070. [[CrossRef](#)]
10. Fung, B.M.; Khitritin, A.K.; Ermolaev, K. An improved broadband decoupling sequence for liquid crystals and solids. *J. Magn. Reson.* **2000**, *142*, 97–101. [[CrossRef](#)]
11. Lee, J.S.; Khitritin, A.K. Thermodynamics of adiabatic cross polarization. *J. Chem. Phys.* **2008**, *128*, 114504. [[CrossRef](#)]
12. Dvinskikh, S.V.; Zimmermann, H.; Maliniak, A.; Sandström, D. Separated local field spectroscopy of columnar and nematic liquid crystals. *J. Magn. Reson.* **2003**, *163*, 46–55. [[CrossRef](#)]
13. Burum, D.P.; Linder, M.; Ernst, R.R. Low-power multipulse line narrowing in solid-state NMR. *J. Magn. Reson.* **1981**, *44*, 173–188. [[CrossRef](#)]
14. Berger, S.; Braun, S. *200 and More NMR Experiments: A Practical Course*; Wiley: Leipzig, Germany, 2004.
15. Dvinskikh, S.V.; Furó, I. Nuclear magnetic resonance studies of translational diffusion in thermotropic liquid crystals. *Russ. Chem. Rev.* **2006**, *75*, 497–506. [[CrossRef](#)]
16. Fung, B.M. Liquid crystalline samples: Carbon-13 NMR. In *Encyclopedia of Nuclear Magnetic Resonance*; Grant, D.M., Harris, R.K., Eds.; Wiley: Chichester, UK, 1996; pp. 2744–2751.
17. Dvinskikh, S.V.; Zimmermann, H.; Maliniak, A.; Sandström, D. Measurements of motionally averaged heteronuclear dipolar couplings in MAS NMR using R-type recoupling. *J. Magn. Reson.* **2004**, *168*, 194–201. [[CrossRef](#)] [[PubMed](#)]
18. Dvinskikh, S.V.; Sandström, D. Frequency offset refocused PISEMA-type sequences. *J. Magn. Reson.* **2005**, *175*, 163–169. [[CrossRef](#)] [[PubMed](#)]
19. Saielli, G. Fully Atomistic Simulations of the ionic liquid crystal [C(16)mim][NO₃]: Orientational order parameters and voids distribution. *J. Phys. Chem. B* **2016**, *120*, 2569–2577. [[CrossRef](#)] [[PubMed](#)]
20. Constant, M.; Decoster, D. Raman-scattering—Investigation of nematic and smectic ordering. *J. Chem. Phys.* **1982**, *76*, 1708–1711. [[CrossRef](#)]
21. Fung, B.M.; Poon, C.-D.; Gangoda, M.; Enwall, E.L.; Diep, T.A.D.; Bui, C.V. Nematic and smectic ordering of 4-n-octyl-4'-cyanobiphenyl studied by carbon-13 NMR. *Mol. Cryst. Liq. Cryst.* **1986**, *141*, 267–277. [[CrossRef](#)]
22. McMillan, W.L. Simple molecular model for the smectic A phase of liquid crystal. *Phys. Rev. A* **1971**, *4*, 1238–1246. [[CrossRef](#)]
23. Ganzenmuller, G.C.; Patey, G.N. Charge ordering induces a smectic phase in oblate ionic liquid crystals. *Phys. Rev. Lett.* **2010**, *105*, 137801. [[CrossRef](#)]
24. Gorkunov, M.V.; Osipov, M.A.; Kapernaum, N.; Nonnenmacher, D.; Giesselmann, F. Molecular theory of smectic ordering in liquid crystals with nanoscale segregation of different molecular fragments. *Phys. Rev. E* **2011**, *84*, 051704. [[CrossRef](#)]
25. Klimavicius, V.; Gdaniec, Z.; Kausteklis, J.; Aleksa, V.; Aidas, K.; Balevicius, V. NMR and raman spectroscopy monitoring of proton/deuteron exchange in aqueous solutions of ionic liquids forming hydrogen bond: A role of anions, self-aggregation, and mesophase formation. *J. Phys. Chem. B* **2013**, *117*, 10211–10220. [[CrossRef](#)] [[PubMed](#)]
26. Every, H.A.; Bishop, A.G.; MacFarlane, D.R.; Oradd, G.; Forsyth, M. Transport properties in a family of dialkylimidazolium ionic liquids. *Phys. Chem. Chem. Phys.* **2004**, *6*, 1758–1765. [[CrossRef](#)]
27. Matveev, V.V.; Markelov, D.A.; Ievlev, A.V.; Brui, E.A.; Tyutyukin, K.V.; Lahderanta, E. Molecular mobility in several imidazolium-based ionic liquids according to data of H-1 and C-13 NMR relaxation. *Magn. Reson. Chem.* **2018**, *56*, 140–143. [[CrossRef](#)]
28. Frise, A.E.; Dvinskikh, S.V.; Ohno, H.; Kato, T.; Furo, I. Ion channels and anisotropic ion mobility in a liquid-crystalline columnar phase as observed by multinuclear NMR diffusometry. *J. Phys. Chem. B* **2010**, *114*, 15477–15482. [[CrossRef](#)] [[PubMed](#)]
29. Frise, A.E.; Ichikawa, T.; Yoshio, M.; Ohno, H.; Dvinskikh, S.V.; Kato, T.; Furo, I. Ion conductive behaviour in a confined nanostructure: NMR observation of self-diffusion in a liquid-crystalline bicontinuous cubic phase. *Chem. Commun.* **2010**, *46*, 728–730. [[CrossRef](#)]
30. Cifelli, M.; Domenici, V.; Kharkov, B.B.; Dvinskikh, S.V. Study of translational diffusion anisotropy of ionic smectogens by NMR diffusometry. *Mol. Cryst. Liq. Cryst.* **2015**, *614*, 30–38. [[CrossRef](#)]

31. Saielli, G. MD simulation of the mesomorphic behaviour of 1-hexadecyl-3-methylimidazolium nitrate: Assessment of the performance of a coarse-grained force field. *Soft Matter* **2012**, *8*, 10279–10287. [[CrossRef](#)]
32. Saielli, G.; Voth, G.A.; Wang, Y.T. Diffusion mechanisms in smectic ionic liquid crystals: Insights from coarse-grained MD simulations. *Soft Matter* **2013**, *9*, 5716–5725. [[CrossRef](#)]



© 2018 by the authors. Licensee MDPI, Basel, Switzerland. This article is an open access article distributed under the terms and conditions of the Creative Commons Attribution (CC BY) license (<http://creativecommons.org/licenses/by/4.0/>).